Resistivity induced by a rough surface of thin gold films deposited on mica

Raul C. Munoz*

Department of Physics, Universidad de Chile, Blanco Encalada 2008, Casilla 487-3, Santiago 6511226, Chile

Abstract

A central question regarding thin metallic films is how does the roughness of the film affect its electrical transport properties, when its thickness is comparable to or smaller than the electron mean free path. The drive to build ever-faster circuits generates the drive for miniaturization and VLSI, which poses a pressing need to reach full understanding of electron–rough surface scattering. We review progress in the field that has taken place over the last 5 years.

From the theoretical point of view, the so-called mSXW theory [Munoz et al., J. Phys.: Condens. Matter 11 (1999) L299] was recently published. The increase in resistivity induced by electron–surface scattering is computed using Kubo's linear response theory. The conductivity of the film is determined by the spectral function characterizing the one-particle Green's function describing the electron gas confined within the film. The effect of the rough surface is to modify the self-energy of the electron gas. The conductivity of the film turns out to depend on the height–height autocorrelation function (ACF) that describes the rough surface. It can be written in a closed form if the ACF is described either by a Gaussian or by an exponential.

From the experimental point of view, the tendency to use parameters provided by theory as quantities that must be fitted to describe thin-film resistivity data has been replaced by direct measurements of the surface roughness. The first measurement of the ACF of the rough surface of a 70-nm thick gold film deposited on mica was recently published [Munoz et al., Phys. Rev. B 62 (2000) 4686]. The measurement was performed with a scanning tunneling microscope (STM). Using the data recorded with the STM and the mSXW theory, we reproduced the thickness as well as the temperature dependence of the best resistivity data available for gold films on mica. Theory reproduced the data to within a few percent *without adjustable parameters*.

We report also the first measurement of the increase in resistivity induced by electron–surface scattering in gold films deposited on mica, performed at low temperatures and high magnetic fields.

Keywords: Resistivity; Electron surface scattering; Thin solid films

1. Introduction

A central question regarding thin metallic structures is how does the roughness of the surface that limits the structure affect its electrical transport properties, when one or more of the dimensions that characterize the structure are comparable to or smaller than the mean free path of the charge carriers, what is known as "size effects". At the moment, the half pitch among the lines of the integrated circuits used in building PCs is about 100 nm, and this dimension is expected to decrease to about 20 nm by the year 2018 [1]. This trend towards miniaturization leading to very large-scale integration (VLSI) poses a pressing need to reach full understanding of electron–surface scattering. We review progress in the field that has taken place over the last 5 years.

It seems interesting to note that the first paper concerning size effects was published in 1998 by Stone [2]. However, most of the experimental work carried out during the last 50 years relies on the work of Fuchs [3], later extended by Sondheimer [4,5], in what is now known as the Fuchs–Sondheimer (FS) theory. The FS formalism uses a description of electron transport in a metal that is based upon a classical equation, the Boltzmann transport equation (BTE), proposed in the late

* Tel.: +56 2 696 0148; fax: +56 2 696 7359.
E-mail address: ramunoz@cec.uchile.cl.

19th century:

$$\left(\frac{\partial f}{\partial t}\right)_{\text{COLL}} = \left(\frac{\partial f}{\partial t}\right)_{\text{FIELDS}}$$

Here the term on the left represents the rate of change of the distribution function characterizing a gas of point-like particles due to collisions between the particles; the term on the right represents the rate of change of the distribution function induced by the presence of the external fields. The rate of change of the distribution function due to collisions can be written in terms of the quantity $T(\vec{v}, \vec{v}')$ that describes the probability per unit time that a particle moving with velocity $\vec{v}$ before the collision comes out of the collision travelling with velocity $\vec{v}'$:

$$\left(\frac{\partial f(\vec{v})}{\partial t}\right)_{\text{COLL}} = \int \mathrm{d}^3\vec{v}' T(\vec{v}, \vec{v}')(f(\vec{v}') - f(\vec{v}))$$

where $f(\vec{v})$ is the distribution function, a quantity proportional to the density of particles moving with velocity $\vec{v}$.

The first attempts at introducing quantum mechanics in the theoretical description of electron scattering in crystalline solids were based upon BTE. In order to use a classical theory to describe electron transport, one must assume that the wave-like behavior of electrons is not dominant, and that the effect of quantum mechanics can be accounted for by considering electrons as classical point particles, which are nevertheless endowed with an effective mass m^* (by virtue of being immersed in a crystal lattice instead of in vacuum) and are endowed with spin, as phonons are (spin 0 for phonons, spin 1/2 for electrons). The inclusion of quantum mechanics in this otherwise classical description of electron scattering proceeds by writing a Hamiltonian for the electron–phonon interaction, which allows the calculation of the scattering rate $T(\vec{v}, \vec{v}')$ entering the collision operator by means of Fermi's golden rule, and by using quantum statistics to describe the electron and the phonon population.

1.1. Bloch–Gruneisen resistivity

Following this approach, the Bloch–Gruneisen theory describing the resistivity of a crystalline metal was published in the 1930s, a theory that was remarkably successful. The Bloch–Gruneisen resistivity of a metal $\rho_0(T)$ with a spherical Fermi surface, describes the resistivity arising from electron–impurity scattering and from electron–acoustic phonon scattering, and is given by [6]

$$\rho_0(T) = \rho_{\text{R}} + A\left(1 + \frac{BT}{\theta - CT}\right)\phi\left(\frac{\theta - CT}{T}\right)$$

$$\text{with } \phi(x) = 4x^{-5}\int_0^x \frac{z^5 \exp(z)}{(\exp(z) - 1)^2}\,\mathrm{d}z \qquad (1)$$

where A, B, C and θ are constants (tabulated in the case of gold [6]). The temperature-independent term ρ_{R} known as "residual resistivity", is normally attributed to electron–impurity scattering. The temperature dependence of $\rho_0(T)$ arises from the term contained within the brackets, from electron–acoustic phonon scattering. The integral $\phi(x)$ arises from evaluating the collision operator $\left(\frac{\partial f}{\partial t}\right)_{\text{COLL}}$ in BTE, by computing the transition rate $T(\vec{v}, \vec{v}')$ from the Hamiltonian describing the electron–phonon interaction, using a Fermi–Dirac distribution to describe the electron population, and a Bose–Einstein distribution to describe the phonon population. At low temperatures (close to liquid helium), the phonons are frozen out, and the contribution to the resistivity $\rho_0(T)$ arising from $\phi(x)$ becomes negligible compared to ρ_{R}; hence the resistivity of the sample at low temperatures is dominated by the residual resistivity.

The remarkable success of this approach in the case of crystalline metals and semiconductors depends on the validity of a huge simplification. It is assumed that

$$\left(\frac{\partial f(\vec{v})}{\partial t}\right)_{\text{COLL}} = -\frac{f(\vec{v}) - f_0(\vec{v})}{\tau(\vec{v})}$$

where $f(\vec{v})$ represents the electron distribution function in the presence of the external fields, $f_0(\vec{v})$ represents the equilibrium distribution function (the electron distribution function in the *absence* of external fields) and $\tau(\vec{v})$ is the velocity-dependent relaxation time. This is known as the relaxation time approximation.

Notice that not all electron scattering mechanisms present in crystalline solids are such that the corresponding Boltzmann collision operator can be well represented by a relaxation time. Fortunately, for the case of electron–acoustic phonon scattering, electron–optical phonon scattering in non-polar crystals, electron–neutral impurity scattering and electron–ionized impurity scattering, detailed calculations of $\left(\frac{\partial f}{\partial t}\right)_{\text{COLL}}$ based upon the computation of $T(\vec{v}, \vec{v}')$ from the Hamiltonian describing the electron–scatterer interaction confirm the validity of the relaxation time approximation [7,8]. These calculations proceed by using Fermi's golden rule, as well as the Bose–Einstein distribution for phonons, and the Fermi–Dirac distribution for electrons.

Most of the electron scattering mechanisms known in crystalline solids within the first half of the 20th century could be described by a relaxation time, and did not require a quantum mechanical description of charge transport, where the wave-like behavior arising from wave–particle duality would become dominant. This is, perhaps, the reason that explains why early theories of electron transport based upon the classical BTE—patched-up to describe quantum effects in the manner described—were so successful in the case of crystalline metals and semiconductors. Such situation changed over the second half of the 20th century, with the discovery of a variety of physical phenomena involving systems where the observed macroscopic behavior cannot be explained by BTE; phenomena that can only be explained by using quantum transport theories where the wave-like behavior of the charge carriers is dominant from the outset. To name only a few, there is the scanning tunneling microscope, the discovery

of quantum dots, quantum wells, quantum point contacts, the quantum Hall effect, etc.

Note that if two distinct electron scattering mechanisms for which a relaxation time exists are described by their own relaxation times τ_1 and τ_2, then the change of the electron distribution function per unit time, caused by different scattering events, is the addition of the scattering rates arising from each electron scattering mechanism acting alone. In crystalline solids, scattering mechanisms which can be characterized by relaxation times that are independent of the momentum of the electrons, plus the additivity of the scattering rates, $\frac{1}{\tau} = \frac{1}{\tau_1} + \frac{1}{\tau_2}$, lead naturally to the additivity of the corresponding resistivities $\rho = \rho_1 + \rho_2$. This is known as Mathiessen's rule; it played an important role in the early theories of charge transport in crystalline solids.

1.2. Fuchs–Sondheimer theory

Since a relaxation time had not been found to represent the collision operator arising from electron–surface scattering, FS introduced a phenomenological parameter R (the surface reflectivity), as a boundary condition that must be satisfied by the electron distribution function. FS assumed that a fraction $0 \leq R \leq 1$ of the electrons colliding with the rough surface undergo specular scattering, e.g. reverse their momentum perpendicular to the plane that describes the (average) surface upon colliding with it, while the in-plane momentum remains unchanged. The FS result for the increase in resistivity induced by electron–rough surface scattering in a film of thickness t limited by two rough surfaces having the same specularity R is customarily written as a ratio between two conductivities $\frac{\sigma}{\sigma_0}$. Here σ represents the conductivity of the metallic film *including electron–rough surface scattering*, and σ_0 represents the conductivity *of the bulk, i.e., the conductivity that would be observed in the film if electron–surface scattering was switched off*. The FS result is

$$\frac{\sigma}{\sigma_0} = 1 - \frac{3\ell}{2t}(1-R)\int_0^{\pi/2} \frac{\cos\vartheta \sin^3\vartheta \left[1 - \exp\left(\frac{-t}{\ell\cos\vartheta}\right)\right]}{1 - R\exp\left(\frac{-t}{\ell\cos\vartheta}\right)} \mathrm{d}\vartheta \tag{2}$$

Note that the FS result contains two parameters that are *unknown a priori*, the bulk conductivity σ_0 and the corresponding bulk mean free path ℓ.

1.3. Comparison between theory and experiment

The method of data analysis that has been used for several decades to compare theory and experiment, based upon FS theory, is the following:

(a) Prepare a family of thin metallic films of different thickness, evaporating the same material onto similar substrates, keeping *the same conditions of evaporation* (vacuum, temperature of the substrate, speed of evaporation, post-evaporation annealing, if any).

(b) Measure the transport coefficients (resistivity, Hall voltage, magnetoresistance, thermoelectric power, etc.) of each member of the family. The transport coefficient most commonly measured is the resistivity of the films.

(c) Adjust the parameters provided by theory (surface specularity R, bulk conductivity σ_0, bulk mean free path ℓ, r.m.s. surface roughness amplitude δ, in the case of modified versions of FS), until reaching an optimum description of the data (e.g., a description of the temperature dependence and the thickness dependence of the resistivity of a family of thin metallic films, prepared under similar conditions of evaporation).

There are two assumptions that underlie this method of data analysis:

(i) It is assumed that the reflectivity R is independent of the angle between the momentum of the incoming electron and the normal to the surface. It is also assumed that R is common to all members of the family (prepared under similar conditions of evaporation). Therefore R is independent of the thickness of the samples.

(ii) It is assumed that the other parameters provided by theory (σ_0, ℓ, δ) are also independent of the thickness of the sample.

1.4. Conceptual difficulties arising when applying FS theory

The first and most obvious difficulty has to do with the morphology of the films. In the case of gold films deposited on mica, at the very early stages of evaporation, the film consists of isolated islands, whose lateral dimensions depend on the conditions of evaporation. Electrical continuity of the film is achieved once the islands grow sufficiently such that contact is established between neighboring islands. However, although the islands can be considered as crystallites that grow with direction [1 1 1] oriented perpendicular to the surface of the mica [9], different crystallites need not exhibit the same crystalline orientation. This gives rise to grain boundaries between neighboring crystallites which might be partially reflecting. A gold film that exhibits continuity might also contain pinholes and dislocations, as a result of imperfect gold coverage of the substrate, and of lattice mismatch between the gold and the mica. Consequently, the resistivity measured on a thin gold film deposited on mica (a film is considered *thin* when its thickness is comparable to or smaller than the electron mean free path) will normally include contributions arising from electron scattering by defects such as pinholes, grain boundaries and dislocations, which are *not* included in FS theory, nor in other theories of size effects.

Before comparing thin-film resistivity data with theories of size effects, great care must be taken to minimize the contributions to the film resistivity arising from electron scattering by defects other than the rough surfaces. As stated in

a review article assessing the literature published up to the early 1980s concerning the problem of size effects, "... the most important conclusion is that there are virtually no studies on the resistivity of thin metal films from which useful values of $\rho_0\ell_0$ [the product of the bulk resistivity and bulk mean free path] may be deduced. ... It appears that there has been a large amount of experimental work which, because of the ease of production and measurement of thin films, has suffered from the lack of quantification of the properties of the films in terms of grain size and crystallinity as well as almost total lack of appreciation of the complexities of the problem." (Ref. [10, p. 330]).

The second conceptual difficulty arising from FS theory, that has been largely ignored by researchers in the field, is that in the limit of ultrathin films $\left(\frac{\ell}{t} \rightarrow \infty\right)$, the FS conductivity diverges as $\ln\left(\frac{\ell}{t}\right)$ in Eq. (21) of Ref. [5]. In this limit, the conductivity is limited only by electron–rough surface scattering. It follows that, within FS theory, in thin ultrapure films, electron–surface scattering *does not dissipate energy, since it gives rise to a null resistivity*. This limit is wrong, and the error is a consequence of ignoring quantum effects within a classical theory.

A report of the resistivity measured at 4 K in ultrathin films of $CoSi_2$ grown onto n-Si (1 1 1) [11] pose an additional difficulty. The silicide film is a metal. Because of the small (1.2%) lattice mismatch between $CoSi_2$ and Si, and as a consequence of the 600 °C needed to produce the solid reaction between Co and Si, $CoSi_2$ grows on Si (1 1 1) as an almost perfect epitaxial film. Ultrathin films with thickness ranging from 1 to 110 nm have been grown. The new interesting result is that the residual resistivity observed in films with a thickness under 10 nm grows rapidly with decreasing film thickness, in a way that cannot be described by the FS theory, *no matter what specularity parameter is chosen to describe the data* [11].

There is, yet, another argument that has been raised pointing to a shortcoming of FS theory, the argument is due to Ziman [12]. As a consequence of wave–particle duality, one would expect the electrons in a metal film to behave as waves characterized by the Fermi wavelength λ_F (in gold, $\lambda_F = 0.52$ nm). Based upon crude arguments stemming from wave optics, one might expect that the surface reflectivity R should depend both on the direction of motion of the incoming electron relative to the (average) surface, as well as on the scale of distances over which corrugations take place. Corrugations occurring over a scale of length that is far greater than λ_F should lead to a specular reflection that therefore contributes very little to increase the resistivity of the film. On the other hand, corrugations taking place over a scale of length comparable to λ_F (to within an order of magnitude) should contribute rather significantly to increase the resistivity of the film. One might hope that a quantum theory of electron–rough surface scattering would incorporate a mechanism to select the scale of distances over which corrugations take place, to account naturally for the wave-like behavior of electrons.

2. Progress in the theoretical description of size effects: quantum transport theories based upon a Hamiltonian formulation of the problem

Over the last 20 years some theories have been published that permit the calculation of the increase in resistivity induced by electron–rough surface scattering, from the knowledge of the parameters that characterize the (average) rough surface. Progress in this area was triggered by the advent of quantum transport theories of charge transport. These theories, rather than assuming the validity of a classical transport equation such as BTE, to later patch it up—by forcefully introducing the correct quantum distributions describing the phonon population and the electron population in Boltzmann collision operator, together with inserting a surface reflectivity R imposed as a boundary condition on the electron distribution function—proceed from a fresh formulation of the problem. A way was found of writing the Hamiltonian for electrons confined within a metallic film bounded by two rough, parallel surfaces, such that the effect of electron–rough surface scattering can be described by a term that adds to the Hamiltonian describing the electrons confined between two flat, parallel surfaces. The effect of this additive term is considered a perturbation, and the conductivity is computed using a perturbative approach. There is the theory of Trivedi and Aschroft (TA [13]), the theory of Tesanovic, Jaric and Maekawa (TJM [14]) and the theory of Sheng, Xing and Wang (SXW [15]). What these theories have in common is that in all of them, the description of electron transport in terms of BTE was abandoned; they are all quantum theories of charge transport that proceed from a fresh Hamiltonian formulation of the problem, where the effect of electron–rough surface scattering is described by one additional term in the Hamiltonian. We will focus on the SXW theory, for it has two distinct advantages: (a) it is the only quantum transport theory that goes over the FS theory, in the case of thick films where electrons exhibit a short mean free path; (b) it coincides with the TA and TJM theories, within the appropriate limits [13–15].

2.1. The theory of Sheng, Xing and Wang (SXW)

Within the formalism proposed by SXW, the increase in resistivity induced by electron–rough surface scattering is computed using Kubo's linear response theory. The conductivity of the film is calculated from the spectral function characterizing the one-particle Green's function describing the electron gas confined within the film. The effect of the rough surface is to modify the self-energy of the electron gas. The self-energy is computed using the Feymann–Dyson perturbation approach.

To summarize results published by SXW relevant to the present discussion, the ratio of the film conductivity σ to bulk conductivity σ_0 is computed in terms of the quantum reflectivity $R(k_\parallel)$ given by

$$R(k_\parallel) = \left(\frac{1 - k_Z Q(k_\parallel)}{1 + k_Z Q(k_\parallel)}\right)^2 \tag{3}$$

(from Eq. (7) of Ref. [15]) where $Q(k_\parallel)$ represents the dissipative part of the self-energy of the electron gas due to electron-surface scattering, $k_Z^2 = k_F^2 - k_\parallel^2$, where k_F stands for the Fermi momentum and $k_\parallel = (k_x, k_y)$ represents the in-plane momentum. The ratio of the film conductivity σ to bulk conductivity σ_0 is computed in terms of the reflectivity R:

$$\frac{\sigma}{\sigma_0} = 1 - \frac{3}{2}\frac{\ell}{t}\frac{1}{X_0 N_c}\sum_{n=1}^{N_c} u_n \times (1 - u_n^2)\frac{(1 - R(u_n))(1 - E_d(u_n))}{1 - R(u_n)E_d(u_n)} \tag{4}$$

(Eq. (11) of Ref. [15]) where t is the film thickness, ℓ the carrier mean free path in the bulk, $u_n = \frac{q_n}{k_F} = \cos\theta_n = \frac{n\pi}{tk_F}$, $X_c = \frac{tk_F}{\pi}$, $N_c = \mathrm{int}(X_c)$ where $\mathrm{int}(M)$ stands for the integer part of M, $X_0 = \frac{3}{2}\left[1 - \frac{1}{3}\left(\frac{N_c}{X_c}\right)^2\left(1 + \frac{1}{N_c}\right)\left(1 + \frac{1}{2N_c}\right)\right]$ and $E_d(u_n) = \exp\left(\frac{-t}{u_n \ell}\right)$. Eq. (4) is the quantum version of Eq. (2), where the integration over the solid angle $\mathrm{d}\Omega \sim \sin\theta\,\mathrm{d}\theta$ in Eq. (2) has been replaced by a finite sum over the N_c electronic states of a particle in a box which are occupied, states where the perpendicular momentum $q_n = \frac{n\pi}{t}$ is quantized as a result of the confinement of the electron gas between two parallel potential barriers.

A consequence of the quantum formulation of the problem is that the film conductivity no longer diverges in the limit $\left(\frac{\ell}{t} \to \infty\right)$; it remains finite. In the case of a constant reflectivity $R < 1$ (independent of the direction of motion of the electron approaching the rough surface), the surface-limited conductivity σ_s predicted by SXW theory, in the limit $\left(\frac{\ell}{t} \to \infty\right)$, is given approximately, by $\sigma_s = \sigma_0 \frac{3t}{4\ell}\frac{1-R}{1+R}\ln(N_c)$ [16].

To complete the presentation of SXW results relevant to the present discussion, the electron self-energy $Q(k_\parallel)$ is given by

$$Q(k_\parallel) = -\mathrm{Im}\int \frac{\mathrm{d}^2 q_\parallel}{(2\pi)^2} F(k_\parallel - q_\parallel)\bar{q}\cot(t\bar{q}) \tag{5}$$

(Eq. (5) of Ref. [15]) where $\mathrm{Im}(C)$ stands for the imaginary part of a complex number C, $\bar{q} = \left(q_z^2 + \mathrm{i}\frac{k_F}{\ell}\right)^{1/2}$ is a complex wavenumber (introduced to account for the finite conductivity in the bulk), and $F(k_\parallel)$ is the Fourier transform of the height–height ACF $f(r_\parallel)$ averaged over the rough surface, defined by

$$f(r_\parallel) = f(x, y) = S^{-1}\int_S h(a_\parallel)h(a_\parallel + r_\parallel)\,\mathrm{d}^2 a_\parallel \tag{6}$$

where $r_\parallel = (x, y)$ stands for the in-plane coordinates and $h(r_\parallel) = h(x, y)$ represents the random height characterizing the rough surface at position (x, y) with respect to the average (flat) surface at $z = t$ or $z = 0$.

However, SXW used the so-called white-noise approximation, where the ACF $f(x, y)$ is assumed to be proportional to a delta function $\delta(x, y)$ and consequently, its Fourier Transform $F(k_\parallel)$ is a constant independent of the in-plane momentum $k_\parallel$. The white-noise approximation severely limits the predicting power of the theory, for the increase in resistivity induced by electron–rough surface scattering turns out to depend on Q_0, the self-energy of the electron gas confined by rough surfaces such that the Fourier transform of its height–height ACF is well represented by a constant (independent of the in-plane momentum). The undesirable consequence of such approximation is that the measurable properties of the surface become absorbed into this constant.

2.2. *Modified SXW theory (mSXW)*

In order to improve the predicting power of the SXW formalism, we abandoned the white-noise approximation. We computed the self-energy $Q(k_\parallel)$ from Eq. (5), when the average ACF that characterizes the surface is described by a Gaussian $f(x, y) = \delta^2 \exp\left[-\frac{x^2+y^2}{\xi^2}\right]$, or by an exponential $f(x, y) = \delta^2 \exp\left[-\frac{\sqrt{x^2+y^2}}{\xi}\right]$, where (δ, ξ) are the r.m.s. roughness amplitude and lateral correlation length, respectively. Since the corresponding Fourier transforms are real, the main contributions to $Q(k_\parallel)$ arise from the poles of the unperturbed Green's function $\cot(t\bar{q})$ describing an electron gas confined between two flat parallel plates separated by a distance t that can be evaluated using a Mittag–Leffler expansion of $\bar{q}\cot(t\bar{q})$ leading, in the case of a Gaussian ACF, to

$$Q(k_\parallel) = \frac{\xi^2\delta^2}{2t}\pi \exp\left[-\frac{\xi^2}{4}(k_\parallel^2 + k_F^2)\right]\sum_{n=1}^{N_c}\left(\frac{n\pi}{t}\right)^2 \times \exp\left[\left(\frac{n\pi}{t}\right)^2\frac{\xi^2}{4}\right] I_0\left(\frac{\xi^2}{2}k_\parallel\sqrt{k_F^2 - \left(\frac{n\pi}{t}\right)^2}\right) \tag{7}$$

where $I_0(x)$ stands for the modified Bessel function of order zero [17].

In the case of an exponential ACF we obtain, in the limit $\frac{\xi^2 k_F}{\ell} \ll 1$:

$$Q(k_\parallel) = \frac{2\xi^2\delta^2}{t}\sum_{n=1}^{N_c}\left(\frac{n\pi}{t}\right)^2 \times \frac{E[r^2(k_\parallel, q_n)]}{[1 + \xi^2(k_\parallel - q_n)^2]\sqrt{1 + \xi^2(k_\parallel + q_n)^2}} \tag{8}$$

with

$$r^2(k_\parallel, q_n) = \frac{4\xi^2 k_\parallel q_n}{1 + \xi^2(k_\parallel + q_n)^2}$$

where $E(r^2)$ stands for the elliptic integral of second kind [17].

2.3. Increase of resistivity induced by a fractal surface

A report was recently published, where the surface roughness of gold films deposited on mica substrates was measured with an atomic force microscope (AFM). The conclusion of this work is that the roughness of the gold films deposited on mica can be described as a self-affine fractal [18]. For this reason, we extended the mSXW formalism to include the case of fractal surfaces characterized by three parameters: the r.m.s. roughness amplitude δ, the lateral correlation length ξ and the roughness (Hausdorff) exponent H that describes the local fractal dimension, $0 \leq H \leq 1$. Extension of the mSXW formalism to the case of electron scattering by rough fractal surfaces leads to a self-energy of the electron gas given by [19]

$$Q(H, k_{\|}) = \frac{\pi\delta^2\xi^2}{t} \sum_{n=1}^{N_c} \left(\frac{n\pi}{t}\right)^2 \frac{F(1+H, 1/2, 1; z)}{\left[1 + A\xi^2(k_{\|} + q_n)^2\right]^{1+H}}$$

where the function $F(a, b, c; z)$ is the confluent hypergeometric function given by [19]

$$F(a, b, c; z) = \frac{\Gamma(c)}{\Gamma(b)\Gamma(c-b)} \times \int_0^1 t^{-1/2}(1-t)^{c-b-1}(1-tz)^{-a}\,\mathrm{d}t, \quad \mathrm{Re}(c) > \mathrm{Re}(b) > 0$$

and A is a normalization constant given by the self-consistent solution of

$$A = \frac{1}{2H}\left[1 - \left(1 + Ak_C^2\xi^2\right)^{-H}\right]$$

where $k_C = \frac{\pi}{a_0}$ is the upper cutoff wavevector in Fourier space, with a_0 denoting the distance along the (x, y)-plane chosen to limit the validity of the fractal description of the surface, to account for the granularity of the atoms at short distances [19].

In the process of extending the mSXW formalism to compute the increase in resistivity arising from electron–surface scattering in a metal film bounded by rough fractal surfaces, we found evidence suggesting that Mathiessen's rule might be severely violated, when the electron scattering mechanisms that give rise to the observed film resistivity are electron scattering in the bulk plus electron–rough surface scattering [16]. This should not be surprising, for it is simply a consequence of the fact that electron scattering in the bulk can be well described by a semi-classical theory, a solution of BTE within the relaxation time approximation. Within the classical theory, the fact that the metallic sample takes the form of a thin film (and the electron momentum perpendicular to the film is quantized as a consequence of the confinement of the electron gas between two parallel potential barriers) is irrelevant. Hence, the corresponding resistivity is independent of the identity of the electron states. This is in contrast to electron scattering by a rough surface, which cannot be properly described by a relaxation time and requires instead a quantum description of charge transport. Within this quantum description, the identity of the initial and the final state occupied by the electron before and after being scattered plays an important role, as underlined by the very fact that the contribution to the conductivity (Eq. (4)) involves a sum over the subindex n that identifies the states of a particle in a box which are occupied.

The consequence of this asymmetry between electron scattering in the bulk and electron–rough surface scattering is that the additivity of the scattering rates no longer leads to the additivity of the corresponding resistivities, hence the validity of Mathiessen's rule breaks down [16,19].

3. Progress in the experimental methods used to study size effects

Progress in the experimental methodology regarding size effects was triggered by the invention of scanning probe microscopes capable of measuring surface roughness with atomic resolution, and among these, the scanning tunneling microscope (STM). The availability of a STM, convinced us to abandon the tendency of considering the parameters provided by theory (bulk conductivity σ_0, bulk mean free path ℓ, r.m.s. roughness amplitude δ and its lateral correlation length ξ) as adjustable parameters—a tendency that has dominated the literature for several decades—and compelled us to measure directly the surface roughness of a 70 nm gold film evaporated onto a mica substrate.

The reason for using gold is that its surface will not oxidize. Consequently, the measurement of the surface roughness with the STM can be performed in air. The reason for using a mica substrate is that the roughness contributed by the mica consists of cleavage steps that occur rather infrequently over the scale of length of tens of nanometers to hundreds of nanometers set by the electronic mean free path. Consequently, the increase in the resistivity of the film arising from collisions between the electrons and the gold–mica interface can be safely ignored.

3.1. Measurement of the height–height autocorrelation function

The first measurement of the ACF $f(x, y)$ characterizing the roughness of a gold film 70 nm thick evaporated onto mica preheated to 300 °C in UHV was recently published [9]. We performed measurements of the random height $h(r_{\|})$ characterizing the surface with respect to the average surface at $z = t$. From the data recorded with the STM, we computed $f(x, y)$ according to its definition by Eq. (6), in the scales of 300 nm × 300 nm, 100 nm × 100 nm, 30 nm × 30 nm and 10 nm × 10 nm. The results are displayed in Fig. 1. The FWHM of the peak shown in Fig. 1 was less than 1 pixel in all scales except in the shortest scale of 10 nm × 10 nm (Fig. 1a).

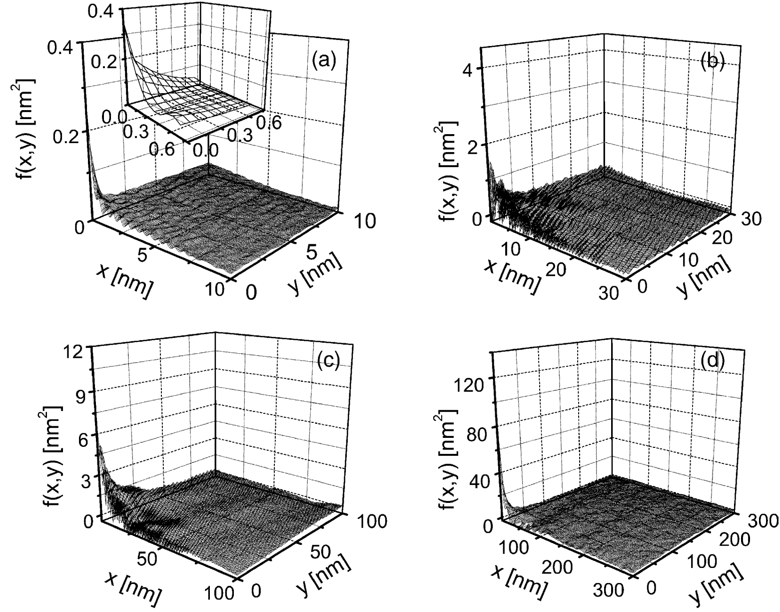

Fig. 1. (a) Average of 20 ACFs calculated from the surface roughness profiles recorded at random locations of the sample on a scale of 20 nm × 20 nm using periodic boundary conditions, from 20 images recorded with the STM containing 256 × 256 pixels each. (x, y) represent the fast and slow scan directions, respectively. The inset shows the details of the 10 × 10 pixels that constitute the central peak of the average ACF. (b) Average of 25 ACFs calculated from the surface roughness profiles recorded at random locations of the sample on a scale of 60 nm × 60 nm using periodic boundary conditions, from 25 images recorded with the STM containing 256 × 256 pixels each. (c) Average of 24 ACFs calculated from the surface roughness profiles recorded at random locations of the sample on a scale of 200 nm × 200 nm using periodic boundary conditions, from 24 images recorded with the STM containing 256 × 256 pixels each. (d) Average of 29 ACFs calculated from the surface roughness profiles recorded at random locations of the sample on a scale of 600 nm × 600 nm using periodic boundary conditions, from 29 images recorded with the STM containing 256 × 256 pixels each. Reprinted from Ref. [9] published by the American Physical Society, with permission.

3.2. The r.m.s. roughness amplitude δ and lateral correlation length ξ: influence of roughness modeling

The data representing the peak at the origin of the average ACF displayed in Fig. 1a was fitted using a Gaussian $f(x, y) = \delta^2 \exp\left[-\frac{x^2+y^2}{\xi^2}\right]$ and an exponential $f(x, y) = \delta^2 \exp\left[\frac{\sqrt{x^2+y^2}}{\xi}\right]$, employing a least-square fit procedure, choosing 6 × 6, 8 × 8, 10 × 10 and 12 × 12 pixels near the origin. The values obtained for δ and ξ, as well as the corresponding values for χ^2 are listed in Table 1 (reprinted from Ref. [20] published by the Institute of Physics Publishing, with permission). The values obtained for δ and ξ are consistent with the atomic resolution exhibited by the tip of the STM when running on HOPG prior to measuring the gold sample. Consequently, the rounding-off that could be expected on the images recorded with the STM due to the finite radius of curvature of the tip does not seem to play a significant role. A glance at Table 1 reveals that both the Gaussian and the exponential provide a good fit (as indicated by the low values of χ^2) to the experimental ACF data, although the fitting by an exponential seems consistently better than the fitting by a Gaussian, for the values obtained for χ^2 are at least a factor of 3 lower. The r.m.s. amplitude δ for the exponential ACF turns out to be about 30% larger than the value corresponding to the Gaussian ACF.

Table 1
Parameters characterizing the ACF data

	Exponential			Gaussian		
	δ	ξ	χ^2	δ	ξ	χ^2
6 × 6	0.746	0.198	0.137	0.539	0.344	0.461
8 × 8	0.687	0.231	0.498	0.494	0.401	2.21
10 × 10	0.633	0.271	0.821	0.448	0.489	3.78
12 × 12	0.602	0.299	1.510	0.422	0.549	7.81
$\langle x \rangle$	0.667	0.250		0.476	0.446	

δ = r.m.s. amplitude; ξ = lateral correlation length; χ^2 = chi-square, parameter characterizing the goodness of the fit. Reprinted from Ref. [20], published by the Institute of Physics Publishing, with permission.

3.3. Quantum reflectivity of the rough surface

The quantum reflectivity arising from the roughness measured in the scale of 20 nm × 20 nm predicted by the mSXW formalism is shown in Fig. 2a, calculated using Eqs. (3) and (7) for a Gaussian representation of the ACF using (δ = 0.455 nm, ξ = 0.480 nm), the average of the values for δ and ξ obtained by least-square fitting the peak at the origin of Fig. 1a over the 8 × 8, 10 × 10 and 12 × 12 pixels near the origin. Since the observed FWHM of the central peak of the ACF is less than one pixel in the larger scales,

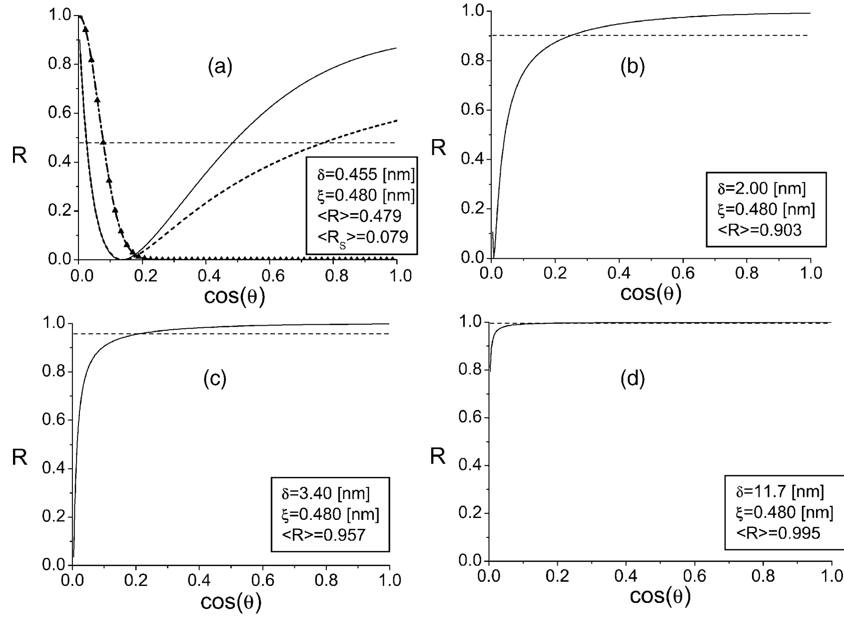

Fig. 2. (a) Reflectivity R characterizing electron–surface scattering predicted by the mSXW theory according to Eqs. (3) and (7), for a film where the average ACF is described by $f(x, y) = \delta^2 \exp\left[-\frac{x^2+y^2}{\xi^2}\right]$, with $\delta = 0.455$ nm, $\xi = 0.480$ nm, plotted as a function of $\cos(\theta)$, where θ represents the angle of incidence between the momentum of the incoming electron and the normal to the surface. The dotted line represents the white-noise reflectivity $R[f_0, \cos(\theta)] = \left[\frac{1-f_0\cos(\theta)}{1+f_0\cos(\theta)}\right]^2$ for $f_0 = 7.16$. The horizontal dotted line represents the average reflectivity $\langle R\rangle = 0.479$ predicted by the mSXW-Gaussian model. The triangles-dotted line represents Soffer's reflectivity R_S given by $R_S(\theta) = \exp\left[-\left(\frac{4\pi\delta}{\lambda_F}\cos(\theta)\right)^2\right]$, where $\delta = 0.455$ nm represents the r.m.s. surface roughness. Soffer assumed that the motion of electrons in a metal film is correctly described by a BTE, and introduced the effect of electron–rough surface scattering via boundary conditions similar to those proposed by FS, except that Soffer introduced an ad hoc reflectivity R_S that is assumed to depend on θ in the manner described [Soffer, J. Appl. Phys. 38 (1967) 1710]. (b) Reflectivity R characterizing electron–surface scattering predicted by mSXW theory according to Eqs. (3) and (7), for a film where the average ACF is described by $f(x, y) = \delta^2 \exp\left[-\frac{x^2+y^2}{\xi^2}\right]$, with $\delta = 2.00$ nm, $\xi = 0.480$ nm, plotted as a function of $\cos(\theta)$. The horizontal dotted line represents the average reflectivity $\langle R\rangle = 0.903$. (c) Reflectivity R characterizing electron–surface scattering predicted by mSXW theory according to Eqs. (3) and (7), for a film where the average ACF is described by $f(x, y) = \delta^2 \exp\left[-\frac{x^2+y^2}{\xi^2}\right]$, with $\delta = 3.40$ nm, $\xi = 0.480$ nm, plotted as a function of $\cos(\theta)$. The horizontal dotted line represents the average reflectivity $\langle R\rangle = 0.957$. (d) Reflectivity R characterizing electron–surface scattering predicted by mSXW theory according to Eqs. (3) and (7), for a film where the average ACF is described by $f(x, y) = \delta^2 \exp\left[-\frac{x^2+y^2}{\xi^2}\right]$, with $\delta = 11.7$ nm, $\xi = 0.480$ nm, plotted as a function of $\cos(\theta)$. The horizontal dotted line represents the average reflectivity $\langle R\rangle = 0.995$. Reprinted from Ref. [9] published by the American Physical Society, with permission.

to calculate the reflectivity R arising from the roughness measured in the larger scales, we used a Gaussian representation of the ACF with $\xi = 0.480$ nm for all scales, but $\delta = 2.00$ nm for the scale of 30 nm × 30 nm, $\delta = 3.40$ nm for the scale of 100 nm × 100 nm and $\delta = 11.7$ nm for the scale of 300 nm × 300 nm. The results are shown in Fig. 2b–d, respectively. The interesting result displayed in these figures is that the angular dependence of the reflectivity changes drastically as the scale of distance (over which the surface roughness is measured) increases, in a way such that the larger the scale of distance, the more the reflectivity R approaches unity. This is also the case if an exponential representation is chosen (instead of a Gaussian) to describe the ACF data.

An interesting prediction of the mSXW formalism concerns the scale of distances over which corrugations take place and their relative contributions to size effects. As illustrated in Figs. 1a–d and 2a–d, the corrugations that determine a specularity R significantly smaller than unity are those taking place over a scale of distances that is large compared with atomic diameter, but small compared with a mesoscopic scale; a scale of distances comparable to λ_F to within one order of magnitude. Electrons colliding with corrugations that take place over mesoscopic scales of distances (tens of nm) or larger have only a minor influence on size effects in gold films. Electrons colliding with such corrugations undergo mostly nearly specular scattering.

The results presented indicate that the mSXW theory is able to select the scale of distance over which corrugations take place, leading to $R \approx 1$ for corrugations taking place over scales of distances which are long when compared to a few λ_F, and $R < 1$ for corrugations taking place over scales of distances which are comparable to λ_F (to within an order of magnitude). The ability of the theory to select the corrugations that take place over a scale of distances which is comparable to λ_F, as the corrugations that actually do contribute to size effects (in the sense that they lead to $R < 1$) is determined by the height–height ACF. As illustrated by Figs. 1a–d and 2a–d, when the amplitude δ grows larger than the wavelength of the carrier λ_F, the reflectivity R increases with increasing δ and it rapidly approaches unity.

3.4. Determination of the bulk conductivity σ_0 and bulk mean free path ℓ

The next issue is how can the roughness parameters (δ, ξ) measured with the STM be used to analyze thin-film resistivity data in a family of metal films of different thickness, dropping the assumption that either the reflectivity R or the bulk mean free path and bulk conductivity (corresponding to each sample) are common to *all* members of the family. Although the contribution arising from electron–phonon scattering is expected to be the same for samples of different thickness, there is no reason a priori why the residual resistivity should also be the same.

The residual resistivity ρ_R appearing in the Bloch–Gruneisen theory (first term in Eq. (1)) depends on the concentration of impurities/defects present in the crystal, and these concentrations *do depend on the preparation of the crystal*. On the other hand, the bulk conductivity σ_0 and bulk mean free path ℓ appearing in FS theory represent the conductivity and mean free path that would be observed in the sample when electron–surface scattering is switched off. Gold films evaporated onto mica substrates exhibit pinholes, dislocations and other defects. If the substrate temperature, vacuum and evaporation speed are kept constant, then the concentration of such defects decreases when the thickness of the sample increases from a few nanometers to some few hundred nanometers. The effect of these defects upon charge transport *will not freeze out upon cooling* as in the case of phonons, hence such defects will influence the residual resistivity of the sample (e.g. the resistivity measured at 4 K).

The calculation of the film conductivity predicted by any of the theories of size effects faces the severe practical difficulty that in order to compute the expected film resistivity $\rho_F(T)$, we need to know the parameters $\sigma_0(T)$ and $\ell(T)$ that characterize the bulk, *and these parameters are not known a priori*. By definition, σ_0 and ℓ correspond to the conductivity and mean free path that would be observed if electron–surface scattering was switched off, i.e., what would be observed in a film thick enough such as to warrant that the effect of electron–surface scattering is negligible, *but a thick film carrying the same concentration of impurities/defects as the sample being measured*. Because the concentration of defects (other than surface roughness) present in gold films evaporated onto mica substrates is observed to depend (among other factors) upon film thickness, such definition of the bulk parameters seems confusing. This has been a stumbling block ever since the very early work by Sondheimer on size effects. To circumvent this difficulty, until now and during several decades, it has been *assumed* that both of these parameters σ_0 and ℓ *are the same for a family of films of different thickness prepared under similar conditions of evaporation*.

Rather than insisting on this unwarranted assumption that seems very difficult to justify, we used a new iteration method that permits the determination of the parameters that characterize the bulk at each temperature T, from the measured film conductivity $\sigma_F(T) = \frac{1}{\rho_F(T)}$ and from the parameters δ and ξ measured with the STM [21]. As a first approximation, $\ell(T)$ corresponding to each temperature T is calculated from $\ell_1(T) = \frac{\sigma(T) m v_F}{n q^2}$, where $\sigma(T) = \frac{1}{\rho(T)}$ is the conductivity of the film measured at temperature T, m is the electron effective mass, v_F is the Fermi velocity, n the electron density and q the electron charge. This value $\ell = \ell_1$ is used to compute a first estimation of $\left[\frac{\sigma(T)}{\sigma_0(T)}\right]_1$, employing the roughness parameters (δ, ξ) to determine the increase in resistivity $\frac{\rho_0(T)}{\rho(T)} = \frac{\sigma(T)}{\sigma_0(T)} = p(T) < 1$ induced by electron–rough surface scattering, according to whichever theory we choose to describe size effects in metal films. A corrected value for ℓ can then be calculated from $\ell_2 = \ell_1 \left[\frac{\sigma_0(T)}{\sigma(T)}\right]_1$, and a new value of $\left[\frac{\sigma(T)}{\sigma_0(T)}\right]_2$ can be computed using the parameters (δ, ξ) and the theory with $\ell = \ell_2$. This process is repeated until the values of $\left[\frac{\sigma(T)}{\sigma_0(T)}\right]_j$ and $\left[\frac{\sigma(T)}{\sigma_0(T)}\right]_{j+1}$ between two successive iterations j and $j+1$ do not differ by more than 0.01% [21].

An interesting situation arises in metal films that satisfy the following conditions: (A) electron–surface scattering taking place at the lower surface of the film (in contact with the substrate) is negligible and (B) the resistivity arising from electron–impurity scattering plus electron scattering by grain boundaries and other defects at 300 K is small compared to that arising from electron–phonon scattering at the same temperature. In samples that satisfy these conditions, the electron scattering mechanisms that give rise to the observed film resistivity are electron–impurity/defect scattering, electron–phonon scattering and electron–surface scattering at the upper surface of the film. The first two scattering mechanisms give rise to the bulk resistivity. For such films, if the theory used to compute the increase in resistivity induced by electron–surface scattering from the parameters (δ, ξ) that characterize the surface roughness is correct, then the temperature-dependent bulk resistivity $\rho_0(T) = \frac{1}{\sigma_0(T)}$ computed through the iteration process outlined above should agree with that expected from electron–phonon scattering plus electron–impurity scattering in the crystalline material. Consequently, the temperature dependence of $\rho_0(T)$ determined according to the iteration process sketched—using as input the film resistivity $\rho_F(T)$ measured at temperature T, and the roughness parameters (δ, ξ) measured with the STM—should be consistent with a Bloch–Grüneisen description of the resistivity $\rho_0(T)$ in the crystalline metal.

But if $\rho_0(T) = \frac{1}{\sigma_0(T)}$ determined through this iteration process turns out, indeed, to be consistent with a Bloch–Grüneisen description, then the observed film resistivity should agree with $\rho(T) = \frac{\sigma_0(T)}{p(T)}$, *where* $\rho_0(T)$*is the bulk resistivity given by* Eq. (1) *and* $(p(T))^{-1}$*represents the increase of resistivity induced by electron–rough surface scattering predicted by theory*. This last criterion provides a very powerful tool to test different theories of size effects in metal films. For if the parameters (δ, ξ) chosen to describe the surface roughness and the theory chosen to describe size effects

are correct, then the theory ought to be capable of describing both *the thickness and the temperature dependence* of the resistivity observed in families of films of different thickness *without adjustable parameters*, something that constitutes quite a stringent test.

3.5. Comparison between different quantum transport theories

Since different theories of electron–surface scattering predict *different values* for $p(T) = \frac{\rho_0(T)}{\rho(T)}$ for the *same* set of parameters (δ, ξ) characterizing the roughness of the surface, it seems interesting to find out if *any* of the available theories describing size effects in metal films is capable of reproducing, at least approximately, the temperature and the thickness dependence of the resistivity data, in samples that satisfy conditions (A) and (B). Concerning condition (A), we expect that electron–surface scattering at the surface of the film in contact with the substrate will be negligible in films that have been grown onto an insulating cleavable crystalline substrate such as mica, for then the roughness contributed by the substrate consists of cleavage steps that occur infrequently over the scale of distance probed by the electrons in their motion through the metal film. Concerning condition (B), we might expect grain boundary scattering to be negligible when the lateral dimension D that characterize the grains that make-up the sample is about one order of magnitude larger than the film thickness t. Sambles, Elsom and Jarvis (SEJ) published measurements of the resistivity of several films of different thickness deposited by thermal evaporation of gold on mica, which led to samples in which D is in the range of several hundred nm (Ref. [22], Fig. 1c and d). The resistivity of the SEJ-35 nm, SEJ-53 nm, SEJ-80 nm and SEJ-126 nm films at 300 K is some 15–30% larger than $\rho_{\text{El-PH}}(300) = 22.5\ \text{n}\Omega\ \text{m}$ expected purely from electron–phonon scattering in crystalline gold [6]; therefore these SEJ samples satisfy conditions (A) and (B).

In order to test the predicting power of the quantum transport theories (TJM, TA, mSXW-Gaussian, mSXW-exponential), and to compare different theories between themselves, we analyzed the best resistivity data available of thin gold films evaporated onto mica substrates, using the roughness parameters (δ, ξ) measured with the STM in the 70 nm gold film evaporated onto mica. We did not succeed in analyzing the resistivity data of the 70 nm gold film, because our film exhibited a resistivity at room temperature of 70 nΩ m, more than three times larger than the resistivity of 22.5 nΩ m due to electron–phonon scattering at 300 K. The increase in resistivity induced by electron–rough surface scattering at room temperature, in our 70 nm gold film, is expected to range between 5 and 20%. This is at variance with the increase of a factor of 3 in the resistivity observed at 300 K, that indicates contamination with impurities and/or defects of unknown origin, that mask the effect of electron–rough surface scattering.

For this reason, we proceeded to analyze the resistivity data published by Sambles et al. [22], employing the new method of data analysis outlined above, and the roughness parameters measured on our 70 nm gold film. The underlying assumption is that our 70 nm film and the SEJ samples exhibit a similar surface roughness, for the surface roughness is controlled by the temperature of the substrate and by the speed of evaporation. When preparing the 70 nm film, we evaporated gold 99.99% pure from a tungsten basket filament at a speed of 6 nm/min in a UHV vacuum system, with the mica substrate preheated to 300 °C. Sambles et al. evaporated their gold 99.9999% pure in a HV vacuum system from a tungsten basket filament, at a speed of 5 nm/min, onto a mica substrate preheated to 270 °C. The outcome of the analysis of the SEJ resistivity data, using the roughness measured on our 70 nm gold film, is displayed in Fig. 3.

The first remarkable result—considering that *none* of the theories contain *any* adjustable parameters—is that all four models provide an approximate description of both the temperature as well as the thickness dependence of the data between 4 and 300 K. Agreement between theory and experiment is about 15% or better in the case of TJM, it is about 10% or better in the case of TA, and it is about 7% or better in the case of mSXW, *regardless of whether we use a Gaussian or an exponential representation of the ACF*. A second interesting feature is that the residual resistivities corresponding to a Bloch–Gruneisen description of the bulk predicted by the *same model are different for films of different thickness*—despite the fact that the films were evaporated under similar conditions of evaporation—and decrease as the thickness of the film increases. This is at variance with the constant residual resistivity (independent of film thickness) that has been assumed for several decades in the analysis of size effect data. This might be expected if thicker films had a smaller concentration of impurities/defects than thinner films, something consistent with the fact that at 4 K, the bulk mean free path ℓ determined using any of the quantum theories grows larger as the film grows thicker. In the case of the mSXW model, the resistivity of the film $\rho(T) = \frac{\rho_0(T)}{p(T)}$ predicted for a Gaussian ACF agrees to better than 0.5% with the resistivity of the film predicted for an exponential representation of the ACF for all four films and $4\ \text{K} \leq T \leq 300\ \text{K}$. It seems reassuring that, within mSXW theory, *both representations of the ACF lead essentially to the same film resistivity*.

The fact that the r.m.s. surface roughness measured on our 70 nm film turns out to be about 17 *times larger* than the value inferred by Sambles et al. from fitting the temperature and the thickness dependence of their data, *using a model containing five adjustable parameters*, underlines the need of revisiting transport measurements on thin metallic films, and the need of cross-checking the parameters characterizing the surface roughness obtained by fitting transport data, with direct measurements of the surface of the films performed on a nanometric scale with a scanning probe microscope capable of atomic resolution [9].

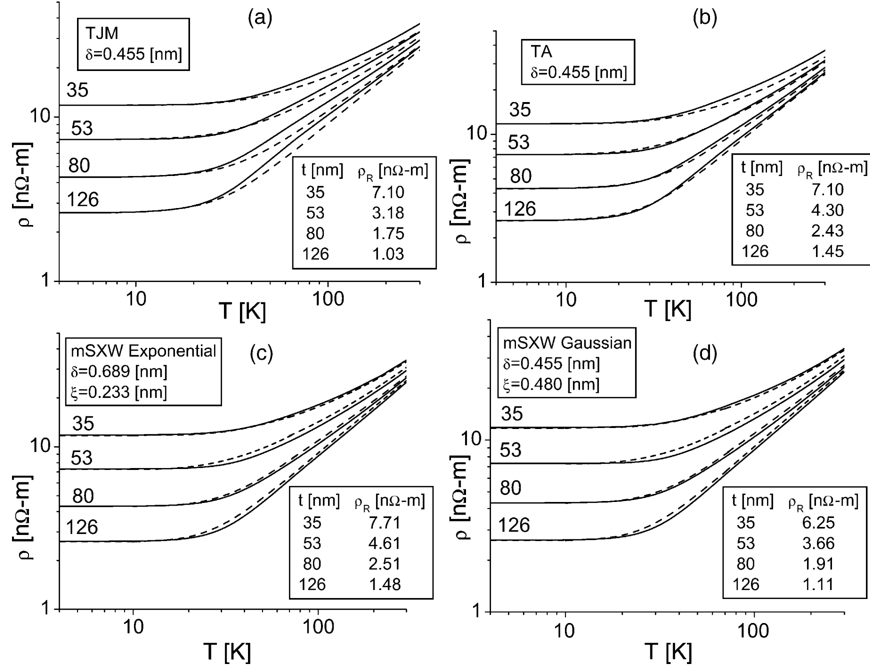

Fig. 3. (a) Dotted line: resistivity of the 35, 53, 80 and 126 nm thick gold films on mica reported in Ref. [22, Fig. 3a]. Solid line: film resistivity $\rho(T)$ described on the basis of a Bloch–Gruneisen model, using Eq. (1), ρ_R as listed, and the constants $A = 12.359$ nΩ m, $B = -9.8996 \times 10^{-4}$; $C = 3.3994 \times 10^{-2}$; $\theta = 172.1$ K from Ref. [6], and using the ratio $\frac{\sigma}{\sigma_0}$ predicted by the theory of Tesanovic, Jaric and Maekawa [14], for an ACF described by a Gaussian with $\delta = 0.455$ nm and $\xi = 0.480$ nm. (b) Dotted line as in (a); Solid line: film resistivity $\rho(T)$ described on the basis of a Bloch–Gruneisen model, using Eq. (1), ρ_R as listed, the constants A, B, C and θ as in (a) and the ratio $\frac{\sigma}{\sigma_0}$ predicted by the theory of Trivedi and Aschroft [13], for an ACF described by a Gaussian with $\delta = 0.455$ nm and $\xi = 0.480$ nm. (c) Dotted line as in (a). Solid line: film resistivity $\rho(T)$ described on the basis of a Bloch–Gruneisen model, using Eq. (1), ρ_R as listed, the constants A, B, C and θ as in (a) and the ratio $\frac{\sigma}{\sigma_0}$ predicted by mSXW theory according to Eqs. (3), (4) and (8), for an ACF described by $f(x, y) = \delta^2 \exp\left[-\frac{\sqrt{x^2+y^2}}{\xi}\right]$ with $\delta = 0.689$ nm, $\xi = 0.233$ nm. (d) Dotted line as in (a); Solid line: film resistivity $\rho(T)$ described on the basis of a Bloch–Gruneisen model, using Eq. (1), ρ_R as listed, the constants A, B, C and θ as in (a) and the ratio $\frac{\sigma}{\sigma_0}$ predicted by mSXW theory according to Eqs. (3), (4) and (7), for an ACF described by $f(x, y) = \delta^2 \exp\left[-\frac{x^2+y^2}{\xi^2}\right]$, with $\delta = 0.455$ nm, $\xi = 0.480$ nm. Reprinted from Ref. [21] published by the Institute of Physics Publishing, with permission.

3.6. *Size effects under a strong magnetic field*

We report below the first measurement of the increase in resistivity induced by electron–surface scattering in gold films deposited on mica, performed at low temperatures and high magnetic fields. Since this seems to be the first measurement of magnetoresistance at low temperatures and high magnetic fields performed on gold films where the signal can be unequivocally attributed to electron–surface scattering, it seems appropriate to briefly review the background to the problem.

The notion that electron–surface scattering *increases* the resistivity of a thin metallic film (in the absence of a magnetic field), because the presence of the rough surface implies an electron scattering mechanism that contributes to dissipate the energy of the electrons, is now widely accepted. The effect of a magnetic field is to produce a curvature of the electron trajectory between scattering events. In thin samples under high magnetic fields, the effect of the magnetic field is expected to result in the electrons sampling the rough surface at a rate that is different from what it would be in the absence of a magnetic field. The energy dissipation induced by electron–rough surface scattering ought to manifest itself in galvanomagnetic phenomena such as Hall effect and magnetoresistance.

Since the discovery of the quantum Hall effect in semiconductor heterostructures, the discovery of giant magnetoresistance in nanostructures involving thin magnetic films, and the discovery of high-temperature superconductors, there have been thousands of papers published on galvanomagnetic phenomena in metals and semiconductors within the last 16 years. However, an important fraction of the work published so far involves either:

(a) nanostructures made up of thin metallic films that include a magnetic metal between two non-magnetic metals that gives rise to the so called giant magnetoresistance, where electron scattering involves the interaction between the electron spin and the local magnetic field present in the sample, or
(b) semiconductor heterostructures, built such that differences of the bandgap among the semiconductors that make up the heterostructure give rise to a two-dimensional electron gas (2 DEG) [23], or
(c) high-temperature superconductors.

Technical advances related to molecular beam epitaxy led to facilities where atomic layers of very pure semiconductor materials can be deposited onto the desired substrate, resulting in heterostructures that give rise to a 2 DEG where charge transport occurs in the ballistic rather than in the diffusive regime. The semiconductor material making up the heterostructure can be made so pure that the electrons move ballistically—without undergoing bulk scattering—from one electrode to the opposite electrode. Under such conditions, charge transport is best described in terms of electron waves that propagate through the cavity defined by the macroscopic boundaries that define the electrodes, according to the quantum formalism proposed by Buttiker and Landauer, to describe the conductance of quantum point contacts in terms of the quantum of conductance q^2/h, where q is the electron charge and h is Planck's constant [23].

A consequence of these developments is that even though there are many hundreds of papers published concerning the increase of resistivity induced by electron–surface scattering in thin metallic films in the absence of a magnetic field, there are only a few papers published addressing size effects in non-magnetic metals in the presence of a magnetic field. The theoretical treatment of size effects in the presence of a magnetic field is scarce [4,5,24]. In fact, a computerized literature search performed on Hall effect or longitudinal or transverse magnetoresistance over the last 16 years, turned up over 6000 articles published during this period. And yet, the treatment proposed by Calecki [24] is the last paper published addressing the simpler problem of galvanomagnetic phenomena and size effects in non-magnetic metals in the presence of a magnetic field, in samples where electron transport occurs in the diffusive rather than the ballistic regime, and the effect of electron–rough surface scattering is expected to increase the (finite) resistivity of the film set by electron scattering in the bulk.

Measurements of the transport coefficients in thin films made out of non-magnetic metals, in the presence of a strong magnetic field at low temperatures (temperatures close to liquid Helium, such as to warrant phonon freeze out and hence long mean free paths and therefore repeated sampling of the rough surfaces) are also very scarce [25].

For the magnetoresistance experiments reported below, we prepared some fresh gold films of different thickness, evaporating gold 99.9999% pure from a tungsten basket filament at a speed of 3 nm/min, onto freshly cleaved mica substrates in an HV evaporation chamber (vacuum of 1.0×10^{-4} Pa or better during evaporation). The mica was preheated to 270 °C before evaporation; the films were annealed for 1 h at 270 °C after evaporation. This time the films did exhibit a resistivity at 300 K that is only a few percent higher than the 22.5 nΩ m expected from electron–phonon scattering in crystalline gold at this temperature. This constitutes an indication that defects such as grain boundaries, pinholes or impurities contribute a minor fraction of the observed film resistivity.

We recorded an X-ray diffractogram of each sample, running a Siemens D-5000 X-ray diffractometer on the θ–2θ mode. In all four samples, the diffractogram yielded a peak at $2\theta = 38.314°$ that corresponds to the [1 1 1] reflection of gold. Therefore, all four samples are made up of grains that coalesced to form the film; the grains grew oriented such that direction [1 1 1] is perpendicular to the surface of the mica.

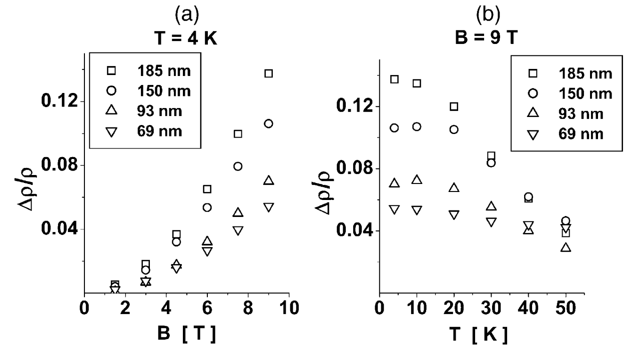

Fig. 4. (a) Dependence of the magnetoresistance $\frac{\Delta\rho}{\rho} = \frac{\rho(B)-\rho(0)}{\rho(0)}$ on the strength of the magnetic field B at a temperature $T = 4$ K. (b) Dependence of the magnetoresistance $\frac{\Delta\rho}{\rho}$ on temperature T, at a magnetic field strength $B = 9$ T.

The dependence of the magnetoresistance on the magnetic field strength B observed at 4 K, with B perpendicular to the sample (along direction [1 1 1] of gold) is shown in Fig. 4a. The dependence of the magnetoresistance on temperature T, at a magnetic field strength of 9 T, is shown in Fig. 4b. The resistivity measured at 4 K was 7.01, 4.72, 3.27 and 2.14 nΩ m on the samples with a thickness of 69, 93, 150 and 185 nm, respectively. At 4 K and 9 T, the product $\omega\tau$ (where ω stands for the cyclotron frequency and τ stands for the average time between collisions within the Drude model—*not a relaxation time*) is 0.14, 0.20, 0.29 and 0.45.

The thickness dependence of the data underlines the fact that electron–rough surface scattering does play a central role in the increase in resistivity induced by the presence of the magnetic field. This is consistent with the fact that, at 4 K, the ratio between mean free path and film thickness is of order 2 in all four samples. The effect of increasing temperature is, as expected, to reduce the time elapsed between scattering events, and hence to reduce the influence of the magnetic field. The relative decrease of $\frac{\Delta\rho}{\rho}$ with increasing temperature is larger for thicker samples. This might be expected from Kohler's rule [26], for thicker samples exhibit a smaller resistivity and hence a larger value for $\omega\tau$, at a given temperature. What seems interesting is the nonlinear dependence of the magnetoresistance on the strength of the magnetic field. The increase of about 14% observed at 4 K and 9 T in the thickest sample seems surprisingly large. A similar nonlinear dependence of the magnetoresistance has been reported on a 110 nm thick film of $CoSi_2$ measured at 4.2 K and 9 T, the observed increase is about 1.5%. The nonlinearity was attributed to the presence of two types of carriers, electrons and holes [25].

On theoretical grounds, using BTE to describe charge transport, it has been shown that a crystalline metal characterized by a perfect spherical Fermi surface leads to a null

magnetoresistance, both when the electric field $\vec{E}$ is perpendicular to the magnetic field $\vec{B}$, and when $\vec{E}$ is parallel to $\vec{B}$ [26]. In crystalline noble metals such as gold, departures of the Fermi surface from a perfect sphere give rise to a magnetoresistance different from zero [26].

The very fact that the observed magnetoresistance is not zero and is thickness-dependent underlines the fact that electron–rough surface scattering plays a central role in determining the magnetoresistance. The nonlinear dependence of the signal on the strength of the magnetic field B could arise out of the non-spherical Fermi surface of gold, which is a property of the bulk material. On the other hand, it could arise from a geometrical effect unrelated to the properties of the bulk, it could arise from the proximity of the rough surfaces limiting the film to within a distance comparable to or smaller than the electron mean free path. In fact, Calecki's theory (based upon BTE, and assuming a spherical Fermi surface) predicts a magnetoresistance that for weak B depends on B^2 [24]. Further analysis is needed to elucidate the origin of the observed magnetoresistance.

4. Summary and conclusions

We have presented in these lines, recent advances concerning the problem of electron–rough surface scattering in gold films deposited on mica. This paper is *not* a review article, nor could it be, given the limitations of space. We simply tried to convey to the reader, and to the participants in the Third San Luis Symposium on Surfaces, Interfaces and Catalysis, a Pan-American Advanced Studies Institute taking place in Mérida, a critical view of progress in the field that has taken place over the last 5 years.

There are a few conclusions that might be drawn from the information presented here. The first is that the apparent agreement reached by some researchers between resistivity data measured on a family of metallic films of different thickness and its theoretical description using theories that employ several fitting parameters could arise from a numerical accident. The outstanding example is the representation of the best thin-film resistivity data on gold films evaporated onto mica substrates published by Sambles et al., using a model containing *five* adjustable parameters: The r.m.s. roughness amplitude used to fit the data is $\delta \approx 0.026\,\text{nm}$, *about one-tenth of an atomic diameter*, while the value measured with the STM in our 70 nm gold film is $\delta = 0.45\,\text{nm}$, about 17 *times larger*. This remarkable discrepancy may be considered as a signal suggesting that, after over a century of research, perhaps our understanding of electron–rough surface scattering is still in its infancy.

In order to make progress in this field, it seems necessary to combine measurements of the transport coefficients of thin metallic films, with independent measurements of the surface roughness in a nanometric scale, performed with a scanning probe microscope capable of atomic resolution. To validate results obtained through numerical fitting of resistivity data, the fitted parameters describing the surface roughness should be contrasted with direct measurements of the surface roughness [9].

Finally, it seems apparent that if there is energy dissipation associated with electron–rough surface scattering, such energy dissipation will manifest itself in other transport coefficients such as Hall voltage, magnetoresistance, thermoelectric power, etc. The new results presented concerning the increase in resistivity induced by electron–rough surface scattering in the presence of a strong magnetic field at low temperatures, require further analysis. The magnetoresistance signal could arise from the non-spherical Fermi surface of gold, or it could arise purely from electron–rough surface scattering (even ignoring the departures of the Fermi surface of gold from a perfect sphere). Such analysis is in progress.

Acknowledgments

This work was supported by FONDECYT under contract 1010481.

References

[1] International technology road map for semiconductors. http://public.itrs.net/files//2003.
[2] I. Stone, Phys. Rev. 6 (1898) 1.
[3] K. Fuchs, Proc. Camb. Phil. Soc. 34 (1938) 100.
[4] E.H. Sondheimer, Phys. Rev. 80 (1950) 401.
[5] E.H. Sondheimer, Adv. Phys. 1 (1952) 1.
[6] R.A. Matula, J. Phys. Chem. Ref. Data 8 (1979) 1147.
[7] J.M. Ziman, Electrons and Phonons, Oxford University Press, London, 1963.
[8] E.M. Conwell, High Field Transport in Semiconductors, Academic Press, New York, 1967.
[9] R.C. Munoz, et al., Phys. Rev. B 62 (2000) 4686.
[10] J.R. Sambles, Thin Solid Films 106 (1983) 321.
[11] P.A. Badoz, et al., Appl. Phys. Lett. 51 (1987) 169.
[12] J.M. Ziman, Electrons and Phonons, Oxford University Press, London, 1963 (Chapter XI).
[13] N. Trivedi, N.W. Aschroft, Phys. Rev. B 38 (1988) 12298.
[14] Z. Tesanovic, M.V. Jaric, S. Maekawa, Phys. Rev. Lett. 57 (1986) 2760.
[15] L. Sheng, D.Y. Xing, Z.D. Wang, Phys. Rev. B 51 (1995) 7325.
[16] R.C. Munoz, et al., J. Phys.: Condens. Matter 15 (2003) L177.
[17] R.C. Munoz, et al., J. Phys.: Condens. Matter 11 (1999) L299.
[18] Z.H. Liu, N.M.D. Brown, A. McKinley, J. Phys.: Condens. Matter 9 (1997) 59.
[19] R.C. Munoz, et al., Phys. Rev. B 66 (2003) 205401–205411.
[20] R.C. Munoz, et al., J. Phys.: Condens. Matter 12 (2000) 2903.
[21] R.C. Munoz, et al., J. Phys. Condens. Matter 12 (2000) 379.
[22] J.R. Sambles, K.C. Elsom, J.D. Jarvis, Philos. Trans. R. Soc. A 304 (1982) 365.
[23] C.W.J. Beenakker, H. Van Houten, Quantum Transport in Semiconductor Nanostructures, in: Solid State Physics, vol. 44, Academic Press, New York, 1991, pp. 1–228.
[24] D. Calecki, Phys. Rev. B 42 (1990) 6906.
[25] J.C. Hensel, et al., Phys. Rev. Lett. 54 (1985) 1840.
[26] J.M. Ziman, Electrons and Phonons, Oxford University Press, London, 1963 (Chapter XII).